ACSNANO
www.acsnano.org
ARTICLE

One-Step Device Fabrication of Phosphorene and Graphene Interdigital Micro-Supercapacitors with High Energy Density

Han Xiao,[†] Zhong-Shuai Wu,*[,†] Long Chen,[‡,§] Feng Zhou,[†] Shuanghao Zheng,[†,⊥,§] Wencai Ren,*[,‡] Hui-Ming Cheng,[‡,∥] and Xinhe Bao[†,⊥]

[†]Dalian National Laboratory for Clean Energy, Dalian Institute of Chemical Physics, Chinese Academy of Sciences, 457 Zhongshan Road, Dalian 116023, P. R. China

[‡]Shenyang National Laboratory for Materials Science, Institute of Metal Research, Chinese Academy of Sciences, 72 Wenhua Road, Shenyang 110016, P. R. China

[§]University of Chinese Academy of Sciences, 19 A Yuquan Road, Shijingshan District, Beijing, 100049, P. R. China

[⊥]State Key Laboratory of Catalysis, Dalian Institute of Chemical Physics, Chinese Academy of Sciences, 457 Zhongshan Road, Dalian 116023, P. R. China

[∥]Tsinghua-Berkeley Shenzhen Institute (TBSI), Tsinghua University, 1001 Xueyuan Road, Shenzhen 518055, P. R. China

Supporting Information

ABSTRACT: **Rational engineering and simplified fabrication of high-energy micro-supercapacitors (MSCs) using graphene and other 2D nanosheets are of great value for flexible and integrated electronics. Here we develop one-step mask-assisted simplified fabrication of high-energy MSCs (PG-MSCs) based on the interdigital hybrid electrode (PG) patterns of stacking high-quality phosphorene nanosheets and electrochemically exfoliated graphene in ionic liquid electrolyte. The hybrid PG films with interdigital patterns were directly manufactured by layer-by-layer deposition of phosphorene and graphene nanosheets with the assistance of a customized interdigital mask, and directly transferred onto a flexible substrate. The resultant patterned PG films present outstanding uniformity, flexibility, conductivity (319 S cm^{-1}), and structural integration, which can directly serve as binder- and additive-free flexible electrodes for MSCs. Remarkably, PG-MSCs deliver remarkable energy density of 11.6 mWh cm^{-3}, outperforming most nanocarbon-based MSCs. Moreover, our PG-MSCs show outstanding flexibility and stable performance with slight capacitance fluctuation even under highly folded states. In addition, our simplified mask-assisted strategy for PG-MSCs is highly flexible for simplified production of parallelly and serially interconnected modular power sources, without need of conventional metal-based interconnects and contacts, for designable integrated circuits with high output current and voltage.**

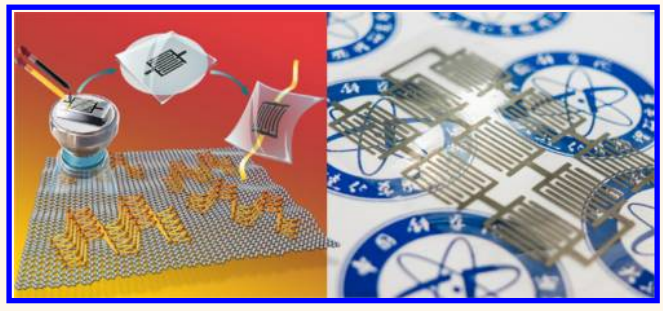

KEYWORDS: *phosphorene, graphene, micro-supercapacitors, ionic liquid, energy storage*

To satisfy the increasing demand of wearable and portable electronics, microscale energy storage devices have spurred intensive attention taking into account that they are lightweight and thin, and have outstanding flexibility, low-cost scalability, and high energy density.[1−3] In this context, planar micro-supercapacitors (MSCs) have the intriguing advantages of high power density, long cycling stability, and fast charge/discharge rate, which are recognized as one of the most promising microscale power sources for integrated electronics.[4−7] Recently, considerable efforts have been devoted to innovating nanostructured materials, including nanocarbons, such as activated carbon,[8] onion-like carbon,[9] carbide-derived carbon,[10] carbon nanotubes (CNTs),[11] graphene,[12,13] and pseudocapacitive materials, such as RuO_2,[14,15] MnO_2,[16] VS_2,[17] polyaniline (PANI),[18] polypyrrole (PPy),[19] polythiophene,[20] and silicon nanowires,[21] as thin-film electrodes for MSCs. Normally, the device manufacturing for typical electrode-patterned MSCs generally involves complicated photolithographic processing (such as spin-coating photoresist, baking, masked irradiation, development), high-pressure

Received: May 11, 2017
Accepted: June 19, 2017
Published: June 19, 2017

DOI: 10.1021/acsnano.7b03288
ACS Nano 2017, 11, 7284−7292

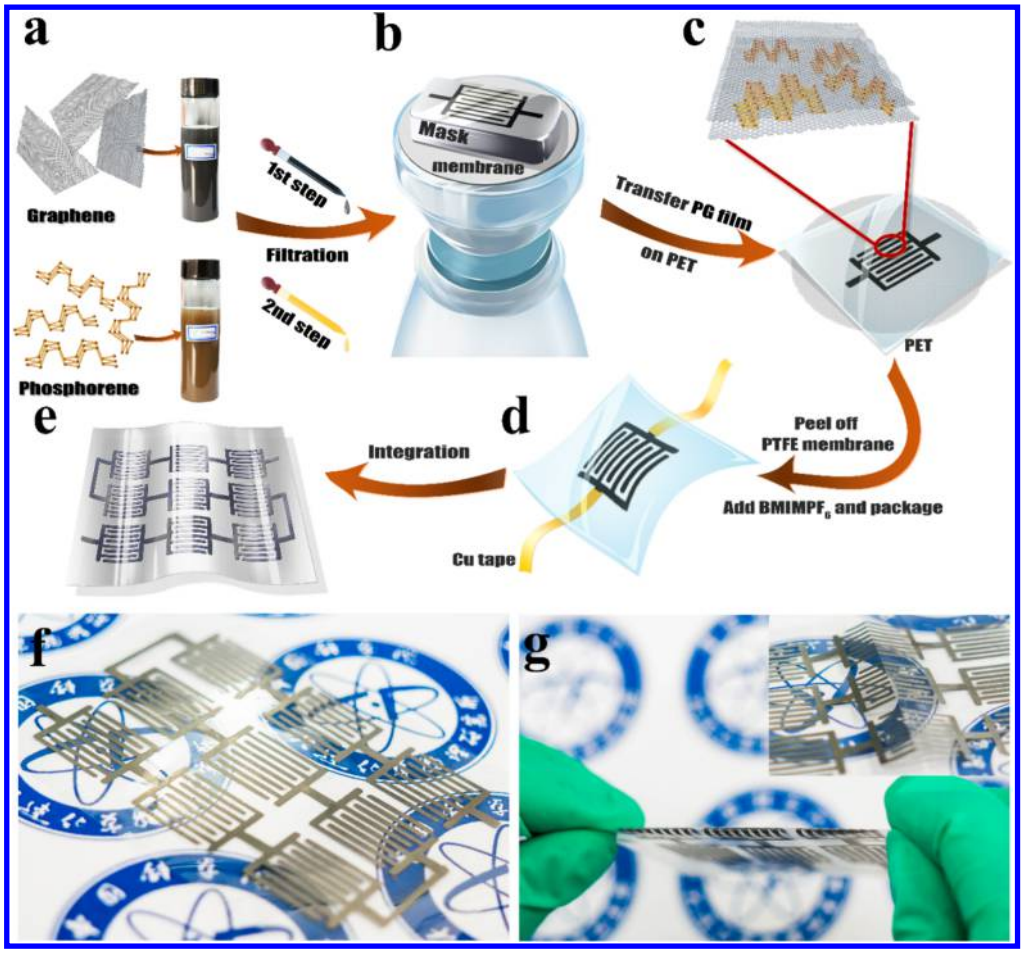

Figure 1. Mask-assisted simplified fabrication of PG-MSCs. (a–e) Illustration of the fabrication of PG-MSCs, which includes the following steps: (a) synthesis of graphene and phosphorene inks; (b) step-by-step filtration of graphene and phosphorene in sequence with the assistance of an interdigital mask; (c) dry transfer of PG hybrid film onto PET substrate; (d) peeling off the PTFE membrane, drop-casting electrolyte, and device package; (e) integration of serially interconnected MSC devices. (f) Photograph of 9 serially interconnected PG-MSCs. (g) Flexibility and stability demonstration of PG interdigital electrodes at a highly folded state. The use of the logo is permitted from Dalian Institute of Chemical Physics, Chinese Academy of Sciences.

pressing, O_2 plasma etching, and sputtering current collectors (e.g., Au).[22−25] So far, several challenges remain in rational engineering of MSCs, such as to (i) develop highly flexible and high-energy electrode materials, including current collectors,[26] (ii) explore high-voltage electrolyte for boosting energy density, and (iii) simplify the device manufacturing process for scalability.[27]

Notably, graphene and other two-dimensional (2D) materials (e.g., MXene) have attracted global attention for creating MSCs with in-plane geometry that can efficiently implement the unique merits of graphene and analogous nanosheets, like atomic thickness and high surface area, for fast on-chip energy storage.[28−33] Because of electric double layer nature of graphene with limited capacitance, one promising strategy for high-performance MSCs is to use graphene-based hybrid films that combine graphene with high conductivity and highly electroactive materials with pseudocapacitance (PANI, PPy, or thiophene).[34−37] Phosphorene, a newly emerging 2D material, has many advantages for energy storage, such as puckered lamellae structure, good electrical conductivity (300 S m^{-1}), thermodynamical stability, large interlayer channel size (3.08 Å), and fast ion diffusion properties. Very recently, several groups have reported the mass production of single- and few-layer phosphorene nanosheets by liquid-phase exfoliation of bulk black phosphorus (BP) in appropriate solvents,[38−40] and demonstrated their applications for lithium ion batteries,[41] sodium ion batteries,[42] and all-solid-state supercapacitors.[43] In particular, Hao et al. reported the fabrication of all-solid-state supercapacitors by using liquid-phase exfoliated few-layer BP nanosheets as flexible electrodes,[43] which have an impressive capacitance of 13.75 F cm^{-3}, outstanding flexibility, and cyclability (15.5% capacitance loss after 10000 cycles). This result shows a great potential of phosphorene for high performance supercapacitors. However, the irreversible reaction of phosphorene with the remnant water of aqueous gel electrolyte was not completely avoided. Nevertheless, the use of phosphorene for planar MSCs has not yet been reported.

Herein, we demonstrate one-step mask-assisted simplified fabrication of high-energy MSCs based on the interdigital electrode patterns of stacking high-quality, few-layer phosphorene nanosheets and electrochemically exfoliated graphene in ionic liquid electrolyte (denoted as PG-MSCs). The PG films with interdigital patterns were directly manufactured through layer-by-layer deposition of phosphorene nanosheets and electrochemically exfoliated graphene with the assistance of a customized mask, and directly transferred onto a polyethylene terephthalate (PET) substrate. The resultant patterned PG films exhibit good uniformity, mechanical flexibility, high

DOI: 10.1021/acsnano.7b03288
ACS Nano 2017, 11, 7284−7292

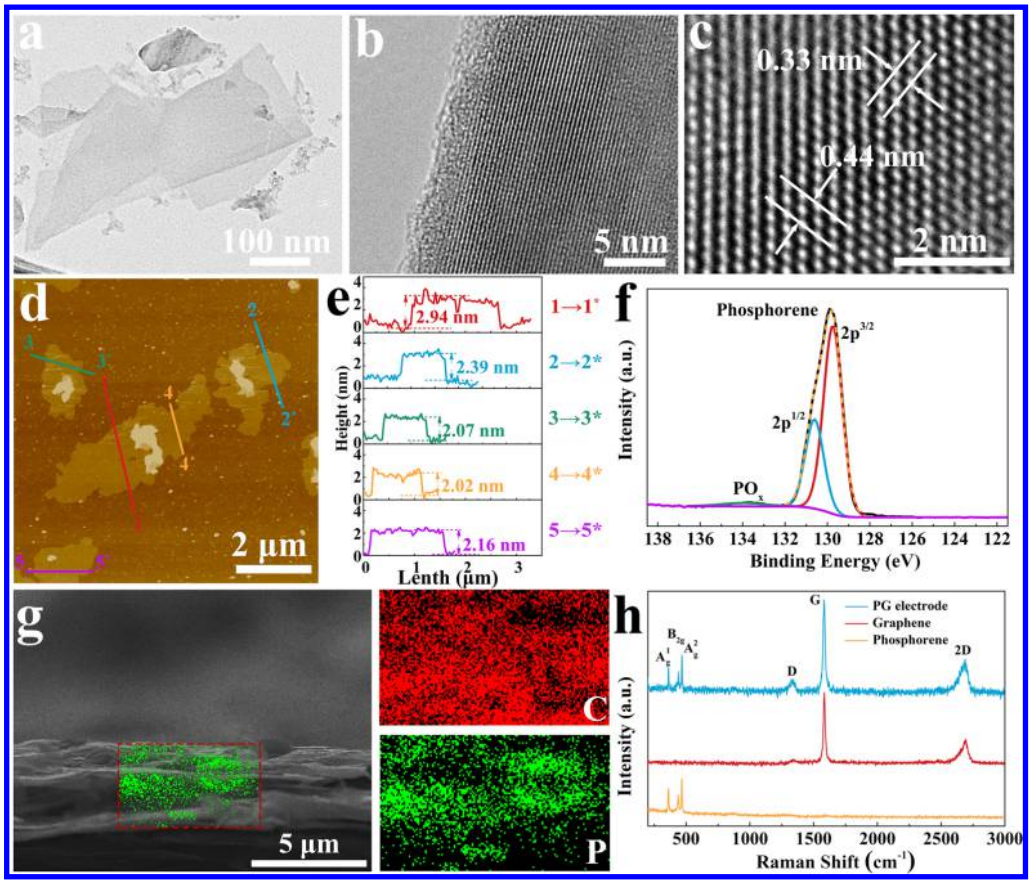

Figure 2. Characterization of phosphorene and PG film. (a) TEM and (b,c) HRTEM images of phosphorene. (d) AFM image and (e) height profiles of phosphorene nanosheets on a silicon wafer. (f) XPS spectrum of phosphorene. (g) Cross-section SEM image of PG film (left) and the corresponding EDX mapping of C and P elements, taken from the square region. (h) Raman spectra of PG film, graphene, and phosphorene.

conductivity (319 S cm^{-1}) and excellent structural integration, which can directly serve as binder- and additive-free flexible electrodes for MSCs. Notably, the PG-MSCs working in ionic liquid of 1-butyl-3-methylimidazolium hexafluorophosphate ($BMIMPF_6$) delivered outstanding areal capacitance of 9.8 mF cm^{-2}, volumetric capacitance of 37.0 F cm^{-3}, and remarkable energy density of 11.6 mWh cm^{-3}. This energy density is at least twice higher than those of the most nanocarbon-based MSCs. Moreover, our PG-MSCs exhibited excellent flexibility and very stable performance without capacitance fluctuation even under highly folded states. In addition, our simplified mask-assisted strategy for PG-MSCs is highly flexible for scalable production of parallelly and serially interconnected modular power sources, without need of conventional metal-based interconnects and contacts, for designable integrated circuits with high output current and voltage.

RESULTS AND DISCUSSION

The mask-assisted fabrication of PG-MSCs is illustrated in Figure 1. First, the high-quality nanosheets of graphene and phosphorene were synthesized. Specifically, graphene was synthesized by an electrochemical cathodic exfoliation process,[44] which possessed large lateral size (10 μm), exceptional conductivity, and high solution processability. In parallel, high-quality phosphorene nanosheets were synthesized in water by liquid-phase exfoliation of bulk BP crystals (Figure S1) that were prepared by the mineralizer-assisted gas-phase transformation method (Figure 2, see details in the Methods Section). Transmission electron microscopy (TEM, Figure 2a) of phosphorene nanosheets exhibited transparent and uniform morphology, and the lateral size ranging from submicrometer to several micrometers. High-resolution TEM (HRTEM, Figure 2b,c) images confirmed the distinct crystal lattice and atomic structure of phosphorene nanosheets. The well-defined lattice space of 0.33 and 0.44 nm were observed, corresponding to (100) and (001) plane, implying that the as-exfoliated phosphorene inherited the nature of high-quality BP. Atomic force microscopy (AFM, Figure 2d,e) measurements showed that the thicknesses are 2.0−2.9 nm, corresponding to 3−5 layers. X-ray photoelectron spectroscopy (XPS, Figure 2f) showed a strong peak at 130 eV, representing P 2p of phosphorene, and a weak broad PO_x peak (2.86% of total P) that was attributed to slight oxidation of the phosphorene surface exposed in air.[45] As reported previously, such high-quality phosphorene nanosheets are highly solution-processable for various applications.[38]

Second, the stable inks of electromechanically exfoliated graphene (0.1 mg mL^{-1} in ethanol, 4 mL) and phosphorene (0.1 mg mL^{-1} in deionized water, 4 mL, Figure 1a) were consecutively vacuum filtered through a polytetrafluoroethylene (PTFE) membrane, with the help of an interdigital-patterned customized mask, to form a shape-designable stacked hybrid film (Figure 1b). Top-view scanning electron microscopy (SEM) showed large-area uniformity and continuity of the PG film, and cross-section SEM images (Figures 2g and S2)

DOI: 10.1021/acsnano.7b03288
ACS Nano 2017, 11, 7284−7292

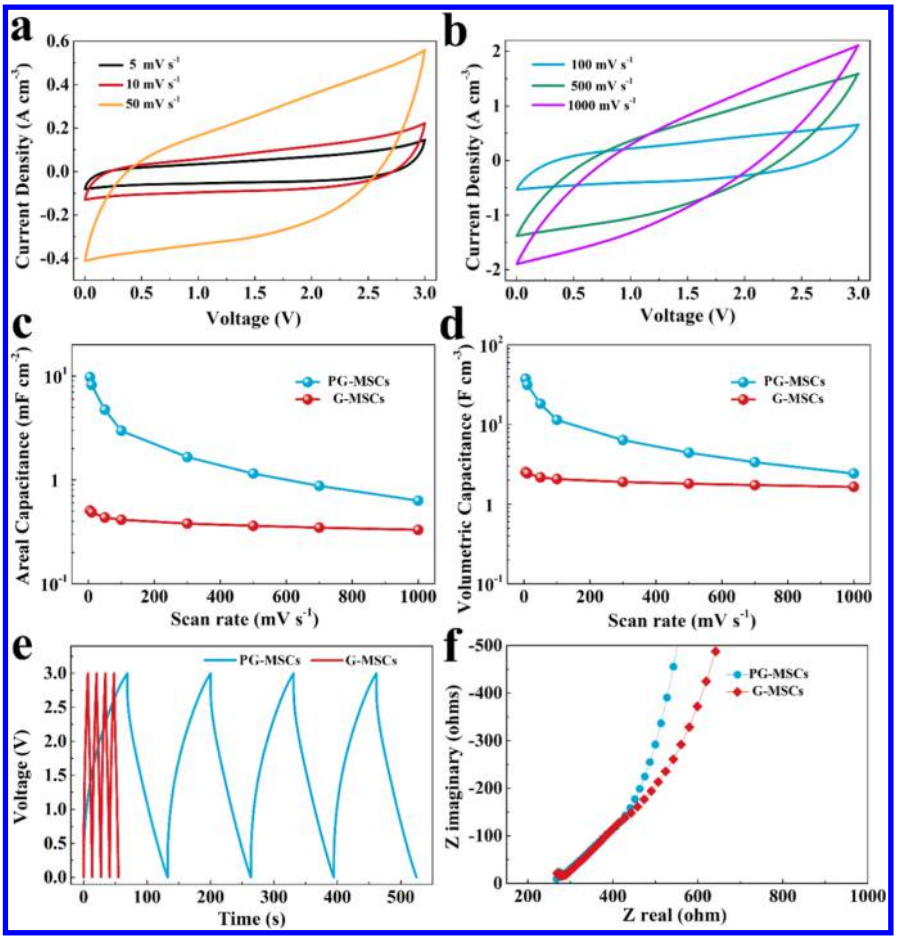

Figure 3. Electrochemical characterization of PG-MSCs and G-MSCs. (a,b) CV curves of PG-MSCs obtained at different scan rates of (a) 5−50 mV s^{-1} and (b) 100−1000 mV s^{-1}. (c) Areal capacitance and (d) volumetric capacitance of PG-MSCs and G-MSCs at different scan rates. (e) GCD curves of PG-MSCs and G-MSCs at current density of 0.3 A cm^{-3}. (f) The complex plane plot of PG-MSCs and G-MSCs.

revealed a compact layered structure of PG film, in which the relatively small phosphorene nanosheets were uniformly incorporated into the interlayer of large graphene nanosheets, as confirmed by energy dispersive X-ray (EDX) mapping analysis (Figure 2g) and our experimental observation (Figure S4). Raman spectra of PG film (Figure 2h) further validated the crystalline nature of phosphorene, with typical A_g^1 (~362 cm^{-1}), B_{2g} (~439 cm^{-1}), and A_g^2 (~466 cm^{-1}) modes,[46] and high quality of graphene, showing a weak D peak and sharp G and 2D peaks.[47] Significantly, the PG film presented a high electrical conductivity of 319 S cm^{-1} (Figure S5), much higher than those of previously reported graphene/polymer hybrid films (21−40 S cm^{-1}).[34,35] Such high conductivity of PG film and layer-stacked structure of phosphorene-incorporated graphene networks can guarantee both high electron transport and fast ionic transport, thus endowing high electrochemical performance.

Afterward, the as-fabricated patterned film was directly dry-transferred onto a PET substrate (thickness of 12.5 μm) (see details in the Methods Section, Figure 1c). After peeling off the PTFE membrane, the PG film with an interdigital pattern was obtained on the thin PET substrate. Finally, after drop casting of ionic liquid ($BMIMPF_6$) and device package, a planar PG-MSC was fabricated (Figure 1d). It is worth it to note that our simplified mask-assisted strategy for PG-MSCs is highly flexible and scalable for the production of serially interconnected MSC pack (Figure 1e−g), without requirement of metal-based interconnects and contacts. More importantly, the as-produced interdigital electrodes of serial PG-MSCs exhibited exceptional mechanical flexibility and superior adhesion to the PET substrate even at a highly bending state, e.g., folded (Figure 1g). No external force-induced shape failure and dimensional disruption was observed, which was assigned to tight stacking and intimate integration of graphene and phosphorene nanosheets in PG films.

The electrochemical performance of PG-MSCs was first measured in 3 V at $BMIMPF_6$ electrolyte by cyclic voltammetry (CV) measurement at different scan rates from 5 to 1000 mV s^{-1} (Figure 3a,b). To highlight the superiority of the layer-structured PG film for MSCs, we also fabricated planar MSCs based on only electrochemically exfoliated graphene films (denoted as G-MSCs), while keeping film processing and cell assembly the same as PG-MSCs. The average thickness of films for PG-MSCs and G-MSCs was evaluated by a surface profiler (Figure S6) to be ~2.0 and ~2.6 μm, respectively. It was observed that CVs of PG-MSCs exhibited a typical capacitive feature with a rectangular shape at low scan rates of 5−50 mV s^{-1} (Figure 3a), and much higher volumetric current density than those of G-MSCs (Figures 3b and S7). The areal capacitance and volumetric capacitance of PG-MSCs and G-MSCs were compared in Figure 3c,d. Notably, PG-MSCs delivered outstanding areal capacitance of ~9.8 mF cm^{-2} and volumetric capacitance of 37.5 F cm^{-3} at 5 mV s^{-1}, both of which were 10 times higher than those of G-MSCs (0.5 mF

DOI: 10.1021/acsnano.7b03288
ACS Nano 2017, 11, 7284−7292

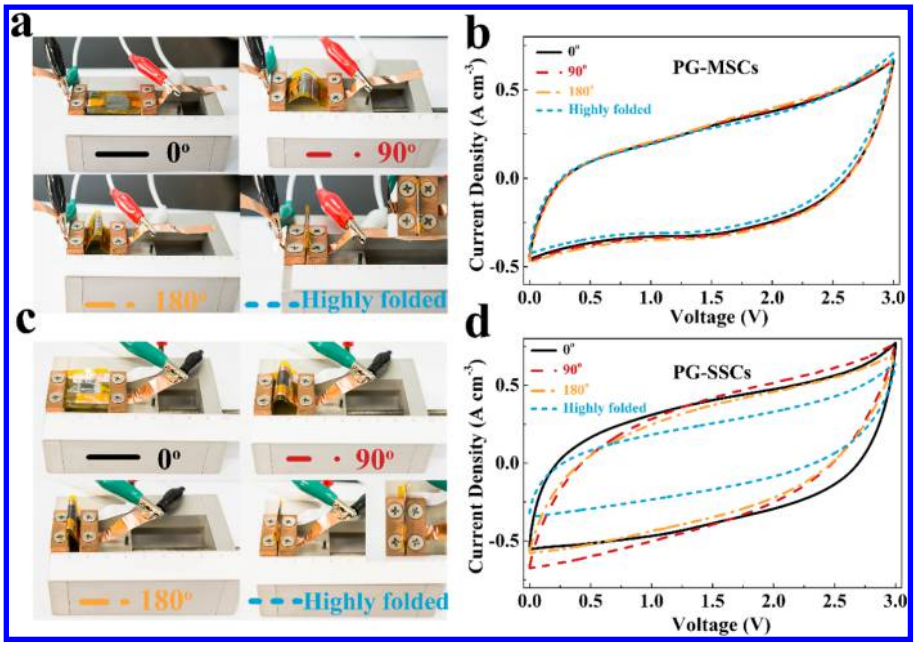

Figure 4. Flexibility comparison of PG-MSCs and PG-SSCs. (a) Photographs of PG-MSCs at different bending states and (b) the corresponding CV curves measured at 100 mV s^{-1}. (c) Photographs of PG-SSCs at different bending states and (d) the corresponding CV curves tested at 100 mV s^{-1}.

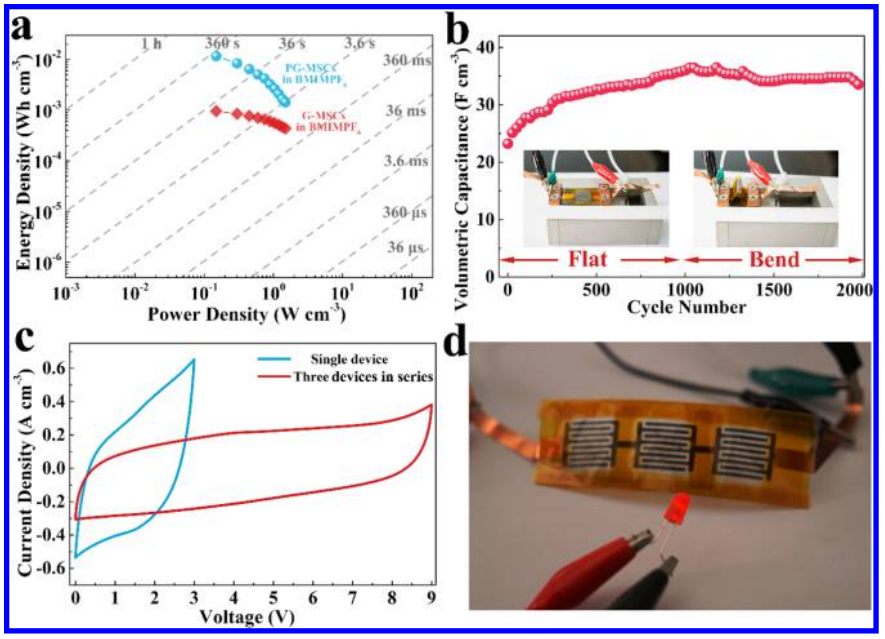

Figure 5. Electrochemical performance of PG-MSCs. (a) Ragone plot of PG-MSCs and G-MSCs. (b) Cycling stability of PG-MSCs obtained at 0.44 A cm^{-3} for 2000 cycles under flat and bending state. The insets are optical images of PG-MSCs in flat and bend states. (c) CV curves obtained at 100 mV s^{-1} of single and three serial PG-MSCs. (d) Photograph of three serial PG-MSCs used to power a light-emitting diode (LED).

cm^{-2} and 2.5 F cm^{-3} at 5 mV s^{-1}), much higher than those of pure phosphorene films for sandwich supercapacitors in aqueous gel electrolyte (2.7 mF cm^{-2} and 17.8 F cm^{-3} at 5 mV s^{-1}), and the most reported nanocarbon-based MSCs without additional metal current collectors (Table S1). Moreover, high capacitances of ∼0.63 mF cm^{-2} and ∼2.42 F cm^{-3} were still retained at a large scan rate of 1000 mV s^{-1}. In a sharp contrast, G-MSCs showed low capacitance of 0.33 mF cm^{-2} and 1.65 F cm^{-3} at 1000 mV s^{-1}. The performance enhancement of PG-MSCs in comparison with G-MSCs was also proven by galvanostatic charge and discharge (GCD) profiles (Figure 3e). Meanwhile, electrochemical impedance spectra (EIS) further disclosed better capacitive behavior of PG-MSCs than that of G-MSCs (Figure 3f), in which the former displayed a larger slope compared with the latter at low frequency. At high frequency region, both of them exhibited comparable equivalent series resistance (ESR) of ∼270 Ω, assigning to the similar resistance of ionic diffusion and interfacial resistance of devices.[48,49] The high resistance is mainly attributed to the low ionic conductivity of ionic liquid

DOI: 10.1021/acsnano.7b03288
ACS Nano 2017, 11, 7284−7292

($BMIMPF_6$, Figure S8).[34] Furthermore, it is worth noting that the film manufacturing and optimization for structural integration of both graphene and phosphorene are key for fully utilizing their conductive and capacitive role, and thus maximizing their performance (Figure S9).

To elucidate the outstanding mechanical flexibility of planar PG-MSCs (Figure 4), we also fabricated traditional sandwich supercapacitors with a separator (Celgard 3501) between two same PG films on PET substrates (denoted as PG-SSCs), and compared their electrochemical performance at different bending states at 0, 90, 180°, and highly folded (Figures 4a,c and S10). Remarkably, all the CV curves of PG-MSCs were almost well overlapped even though the device was highly folded (Figure 4b), demonstrative of superior flexibility and electrochemical stability. In contrast, CV shapes of PG-SSCs substantially declined with increasing bending angle (Figure 4d). For instance, PG-SSCs retained only ~53% of the initial capacitance at a flat state, much lower than that of PG-MSCs (94%), while bended at a highly folded state. The exceptional flexibility of PG-MSCs can be explained by the superiority of interdigital planar device geometry over nonplanar stacked geometry in PG-SSCs. Specifically, in the case of planar PG-MSCs, the interdigital positive and negative electrodes are patterned on a single substrate, and the physical empty interspacing between electrodes can directly serve as a separator, without need of a commercial separator in PG-SSCs. In contrast, the inevitable contact and deformation of the two film electrodes with an ionic separator in a stacked geometry could substantially induce poor ion diffusion and electron transport under bending states, resulting in remarkable performance degradation of PG-SSCs especially at a high curvature state.

The Ragone plot of PG-MSCs compared with G-MSCs were presented in Figure 5a. Remarkably, our PG-MSCs (based on two electrodes) showed a maximum volumetric energy density of ~11.6 mWh cm^{-3} in $BMIMPF_6$ electrolyte, which is much higher than those of G-MSCs (~1.0 mWh cm^{-3}), few-layer phosphorene-based supercapacitors in gel electrolyte (~2.47 mWh cm^{-3}) and most nanocarbon-based MSCs (Table S1), e.g., 2.0 mWh cm^{-3} for laser-scribed graphene,[43,50] 2.5 mWh cm^{-3} for methane plasma reduced graphene,[51] 3.2 mWh cm^{-3} for carbide-derived carbon,[52] 0.6 mWh cm^{-3} for B-doped laser-induced graphene,[53] 1.6 mWh cm^{-3} for onion-like carbon,[9] and 4.0 mWh cm^{-3} for laser-written graphene.[54] Furthermore, PG-MSCs delivered an impressive volumetric power density of 1500 mW cm^{-3}. The cycling stability of PG-MSCs was measured at a current density of 0.44 A cm^{-3} under flat and constant bending state (at 180°) each for 1000 cycles (Figures 5b and S12). It was observed that the volumetric capacitance of PG-MSCs gradually increased from 23.2 to 36.9 F cm^{-3} during the initial stage of ~1200 cycles, and then kept almost stable in subsequent cycling, with about ~89.5% of the maximum capacitance retained after 2000 cycles. This enhanced capacitance is attributed to the dynamical improvement of ion accessibility into the interlayer of the PG film during cycling, leading to an increased accommodation for charge storage.

To further demonstrate the scalability and integration of our manufacturing strategy, three serial PG-MSCs without additional metal-based conductive wires were readily interconnected to form a high-voltage device pack on a single PET substrate. As shown in Figure 5c, the three serially connected PG-MSCs, similar to the single device, exhibited a nearly rectangular CV shape in the voltage extension of 9 V, indicative of excellent performance uniformity. Notably, our serial devices could easily power a LED (Figure 5d), illustrating the great potential for real applications for powering electronics.

The excellent performance of PG-MSCs in ionic liquid is attributed to the synergistic combination of elaborated selection of two types of 2D nanosheets with complementary properties, simplified device fabrication process, strong interfacial engineering between electrode and substrate, and usage of ionic liquid electrolyte. First, the 2D phosphorene and graphene nanosheets in PG films have a strong coupling effect for energy storage. The puckered phosphorene lamellae offer more ionic accommodation and fast transport pathway, and significantly prevent the restacking of graphene sheets, while high-conductive capacitive graphene works as main mechanical skeleton and high-speed electron transport network, guaranteeing efficient utilization of phosphorene nanosheets for energy storage. Second, our simplified device fabrication of PG-MSCs can efficiently avoid the oxidation of phosphorene and solvent contamination originating from multiple-step lithographic processing, e.g., O_2 plasma etching, and photoresist. Moreover, such a simplified manufacturing process is highly flexible for scalable device integration. Third, atomic thickness and mechanical flexibility of 2D nanosheets are favorable for achieving the strong interfacial interaction between phosphorene and graphene nanosheets, as well as film electrode and substrate. In particular, the interdigital electrodes constructed on one coplanar substrate without need of a separator is critical for maximizing charge storage of the 2D nanosheets. Last but not the least, ionic liquid used in our system offers high operating voltage (3 V), avoids the oxidation of phosphorene that easily occurs in aqueous electrolyte during electrochemical process, and has high thermal stability (up to 200 °C), which are essentially important for constructing high-voltage, stable, and safe MSCs.

CONCLUSIONS

In summary, we demonstrated the simplified manufacturing of high-energy PG-MSCs in ionic liquid, based on the mask-assisted directly patterned interdigital electrodes of high-quality phosphorene and graphene. The as-fabricated PG-MSCs combine the advantages of phosphorene and graphene, ionic liquid, strong interfacial interaction, and simplified device fabrication, and consequently displayed outstanding areal capacitance of 9.8 mF cm^{-2} and remarkable energy density of ~11.6 mWh cm^{-3}, outperforming most reported nanocarbon-based MSCs. Moreover, our PG-MSCs showed excellent flexibility with very stable performance under different bending states, and superior integration without metal-based interconnects and contacts. The strategy proposed for the simplified construction of MSCs is readily extended to graphene and analogous nanosheets for flexible, safe, and planar high-performance energy storage devices.

METHODS

Preparation of Phosphorene. Phosphorene nanosheets were prepared by liquid-phase exfoliation of BP crystals as reported previously.[38] Typically, bulk BP crystal was synthesized from red phosphorus, AuSn alloy, and SnI_4 by a mineralizer-assisted gas-phase transformation method. Then the crystal was ground to powders, dispersing in deionized water (100 mL) with an initial concentration of 5 mg mL^{-1} by tip sonication at a power of 300 W (Scientz-IID ultrasonic homogenizer) for 120 min. After the dispersion had settled

DOI: 10.1021/acsnano.7b03288
ACS Nano 2017, 11, 7284−7292

for 12 h, the supernatant was decanted and then centrifuged at 3000 rpm for 30 min (Cence-TG16-WS). Finally, the resulting supernatant was collected for further characterization and film fabrication.

Preparation of Graphene. Graphene was directly exfoliated from graphite in aqueous solution according to a reported electrochemical exfoliation procedure.[44] After freezing drying, the resultant exfoliated graphene nanosheets were dispersed in ethanol by sonication for 30 min to form 0.1 mg mL^{-1} stable ink.

Fabrication of PG-MSCs and G-MSCs. To fabricate this interdigital film electrode, a customized interdigital mask with four fingers (length of 14 mm, finger width of 1 mm) on each side was manufactured to define the patterned geometry. Subsequently, the stable ink of 4 mL ethanol dispersions of graphene (0.1 mg mL^{-1}) was filtered through a PTFE membrane (pore size 0.2 μm) by mask-assisted vacuum filtration. Afterword, 4 mL deoxidizing water dispersion of phosphorene (0.1 mg mL^{-1}) was filtered to form a hybrid PG film on PTFE membrane. Then, the resultant patterned hybrid film was directly dry transferred to a 12.5 μm-thick PET substrate with assistance of 20 MPa pressure to obtain PG interdigital electrodes. To completely remove the residual water and ethanol, PG electrodes were placed into a vacuum oven for 12 h at 60 °C and then transferred into an argon-filled glovebox (MBraun Labstar, with less than 0.5 ppm of oxygen and water). Finally, $BMIMPF_6$ ionic liquid electrolyte was slowly drop-casted onto the surface of interdigital electrodes and the device was packaged by Kapton tape. For comparison, we also fabricated the G-MSCs based on the pure graphene film by one-step filtration of 4 mL graphene dispersion.

Fabrication of PG-SSCs. To fabricate PG-SSCs for flexibility comparison, a square-shaped customized mask with a size of 10.5 mm × 9 mm was used to define the pattern and to adjust the same mass loading as the interdigital PG-MSCs. Using the same mask-assisted filtration, two pieces of PG films were prepared and thus transferred onto PET substrates. After that, PG-SSCs were assembled based on two PG film electrodes sandwiching an electrolyte-immersed Celgard 3501 membrane as separator, and packaged by Kapton tape.

Materials Characterization. The morphology and structure of graphene, phosphorene, BP, PG, and graphene films were characterized by SEM (JSM-7800F), TEM (JEM-2100), Raman spectrometer (LabRAM HR800), AFM (MultiMode 3D microscopy), XPS with an ESCALAB250 (150 W, spot size 500 μm) using Al Kα radiation, and XRD (Empyrean with Cu Kα radiation in the 2θ range from 5 to 80°). The thickness of the films was examined by surface profiler (Veeco Dektak 150). And electrical conductivity of the films was measured by a standard four-point probe system (RTS-9).

Electrochemical Characterization. CV curves at scan rates of 10−1000 mV s^{-1}, GCD profiles at different current densities, and EIS recorded in the frequency range of 0.01 Hz−100 kHz with a 5 mV ac amplitude were performed by CHI760E electrochemical workstation.

ASSOCIATED CONTENT

Supporting Information

The Supporting Information is available free of charge on the ACS Publications website at DOI: 10.1021/acsnano.7b03288.

Additional detailed calculation, figures, and tables about materials characterization, electrochemical characterization (PDF)

AUTHOR INFORMATION

Corresponding Authors

*E-mail: wuzs@dicp.ac.cn.
*E-mail: wcren@imr.ac.cn.

ORCID

Zhong-Shuai Wu: 0000-0003-1851-4803
Wencai Ren: 0000-0003-4997-8870
Xinhe Bao: 0000-0001-9404-6429

Author Contributions

Z.S. Wu, W.C. Ren, H.M. Cheng, and X.H. Bao proposed and supervised the overall project. H. Xiao did the fabrication and electrochemical measurement of MSCs. H. Xiao and Z.S. Wu analyzed the data. L. Chen fabricated the phosphorene. F. Zhou prepared the graphene. S.H. Zheng participated in the materials characterization. H. Xiao, Z.S. Wu, W.C. Ren, H.M. Cheng, and X.H. Bao wrote the paper. All authors discussed the results and commented on the manuscript. All authors have given approval to the final version of the manuscript.

Notes

The authors declare no competing financial interest.

ACKNOWLEDGMENTS

This work was financially supported by the National Natural Science Foundation of China (Grants 51572259, 51325205, 51290273, and 51521091), National Key R&D Program of China (Grants 2016YBF0100100, 2016YFA0200101, and 2016YFA0200200), Natural Science Foundation of Liaoning Province (Grant 201602737), Thousand Youth Talents Plan of China, DICP (Grant Y5610121T3), China Postdoctoral Science Foundation (Grant 2016M601348).

REFERENCES

(1) Zhao, M. Q.; Ren, C. E.; Ling, Z.; Lukatskaya, M. R.; Zhang, C.; Van Aken, K. L.; Barsoum, M. W.; Gogotsi, Y. Flexible Mxene/Carbon Nanotube Composite Paper with High Volumetric Capacitance. *Adv. Mater.* **2015**, *27*, 339−345.

(2) Shao, Y.; El-Kady, M. F.; Wang, L. J.; Zhang, Q.; Li, Y.; Wang, H.; Mousavi, M. F.; Kaner, R. B. Graphene-Based Materials for Flexible Supercapacitors. *Chem. Soc. Rev.* **2015**, *44*, 3639−3665.

(3) Bonaccorso, F.; Colombo, L.; Yu, G.; Stoller, M.; Tozzini, V.; Ferrari, A. C.; Ruoff, R. S.; Pellegrini, V. 2D Materials. Graphene, Related Two-Dimensional Crystals, and Hybrid Systems for Energy Conversion and Storage. *Science* **2015**, *347*, 1246501.

(4) Lamberti, A.; Clerici, F.; Fontana, M.; Scaltrito, L. A Highly Stretchable Supercapacitor Using Laser-Induced Graphene Electrodes onto Elastomeric Substrate. *Adv. Energy Mater.* **2016**, *6*, 1600050.

(5) Gan, S.; Zhong, L.; Gao, L.; Han, D.; Niu, L. Electrochemically Driven Surface-Confined Acid/Base Reaction for An Ultrafast H^+ Supercapacitor. *J. Am. Chem. Soc.* **2016**, *138*, 1490−1493.

(6) Yu, D.; Qian, Q.; Wei, L.; Jiang, W.; Goh, K.; Wei, J.; Zhang, J.; Chen, Y. Emergence of Fiber Supercapacitors. *Chem. Soc. Rev.* **2015**, *44*, 647−662.

(7) Wang, Y. F.; Yang, X. W.; Pandolfo, A. G.; Ding, J.; Li, D. High-Rate And High-Volumetric Capacitance of Compact Graphene-Polyaniline Hydrogel Electrodes. *Adv. Energy Mater.* **2016**, *6*, 1600185.

(8) Durou, H.; Pech, D.; Colin, D.; Simon, P.; Taberna, P. L.; Brunet, M. Wafer-Level Fabrication Process for Fully Encapsulated Micro-Supercapacitors with High Specific Energy. *Microsyst. Technol.* **2012**, *18*, 467−473.

(9) Pech, D.; Brunet, M.; Durou, H.; Huang, P.; Mochalin, V.; Gogotsi, Y.; Taberna, P. L.; Simon, P. Ultrahigh-Power Micrometre-Sized Supercapacitors Based on Onion-Like Carbon. *Nat. Nanotechnol.* **2010**, *5*, 651−654.

(10) Zhao, J.; Jiang, Y.; Fan, H.; Liu, M.; Zhuo, O.; Wang, X.; Wu, Q.; Yang, L.; Ma, Y.; Hu, Z. Porous 3D Few-Layer Graphene-Like Carbon for Ultrahigh-Power Supercapacitors with Well-Defined Structure-Performance Relationship. *Adv. Mater.* **2017**, *29*, 1604569.

(11) Kim, D.; Shin, G.; Kang, Y. J.; Kim, W.; Ha, J. S. Fabrication of A Stretchable Solid-State Micro-Supercapacitor Array. *ACS Nano* **2013**, *7*, 7975−7982.

(12) Zhu, C.; Liu, T.; Qian, F.; Han, T. Y.; Duoss, E. B.; Kuntz, J. D.; Spadaccini, C. M.; Worsley, M. A.; Li, Y. Supercapacitors Based on Three-Dimensional Hierarchical Graphene Aerogels with Periodic Macropores. *Nano Lett.* **2016**, *16*, 3448−3456.

DOI: 10.1021/acsnano.7b03288
ACS Nano 2017, 11, 7284−7292

(13) Yang, X.; Cheng, C.; Wang, Y.; Qiu, L.; Li, D. Liquid-Mediated Dense Integration of Graphene Materials for Compact Capacitive Energy Storage. *Science* **2013**, *341*, 534−537.
(14) Wu, Z. S.; Wang, D. W.; Ren, W.; Zhao, J.; Zhou, G.; Li, F.; Cheng, H. M. Anchoring Hydrous RuO_2 on Graphene Sheets for High-Performance Electrochemical Capacitors. *Adv. Funct. Mater.* **2010**, *20*, 3595−3602.
(15) Ferris, A.; Garbarino, S.; Guay, D.; Pech, D. 3D RuO_2 Microsupercapacitors with Remarkable Areal Energy. *Adv. Mater.* **2015**, *27*, 6625−6629.
(16) Peng, L. L.; Peng, X.; Liu, B. R.; Wu, C. Z.; Xie, Y.; Yu, G. H. Ultrathin Two-Dimensional MnO_2/Graphene Hybrid Nanostructures for High-Performance, Flexible Planar Supercapacitors. *Nano Lett.* **2013**, *13*, 2151−2157.
(17) Feng, J.; Sun, X.; Wu, C. Z.; Peng, L. L.; Lin, C. W.; Hu, S. L.; Yang, J. L.; Xie, Y. Metallic Few-Layered VS_2 Ultrathin Nanosheets: High Two-Dimensional Conductivity for In-Plane Supercapacitors. *J. Am. Chem. Soc.* **2011**, *133*, 17832−17838.
(18) Xue, M. A. Q.; Li, F. W.; Zhu, J.; Song, H.; Zhang, M. N.; Cao, T. B. Structure-Based Enhanced Capacitance: *in Situ* Growth of Highly Ordered Polyaniline Nanorods on Reduced Graphene Oxide Patterns. *Adv. Funct. Mater.* **2012**, *22*, 1284−1290.
(19) Hughes, M.; Shaffer, M. S. P.; Renouf, A. C.; Singh, C.; Chen, G. Z.; Fray, J.; Windle, A. H. Electrochemical Capacitance of Nanocomposite Films Formed by Coating Aligned Arrays of Carbon Nanotubes with Polypyrrole. *Adv. Mater.* **2002**, *14*, 382−385.
(20) Nejati, S.; Minford, T. E.; Smolin, Y. Y.; Lau, K. K. S. Enhanced Charge Storage of Ultrathin Polythiophene Films within Porous Nanostructures. *ACS Nano* **2014**, *8*, 5413−5422.
(21) Dubal, D. P.; Aradilla, D.; Bidan, G.; Gentile, P.; Schubert, T. J.; Wimberg, J.; Sadki, S.; Gomez-Romero, P. 3D Hierarchical Assembly of Ultrathin MnO_2 Nanoflakes on Silicon Nanowires for High Performance Micro-Supercapacitors in Li- Doped Ionic Liquid. *Sci. Rep.* **2015**, *5*, 9771−9780.
(22) Beidaghi, M.; Wang, C. L. Micro-Supercapacitors Based on Interdigital Electrodes of Reduced Graphene Oxide and Carbon Nanotube Composites with Ultrahigh Power Handling Performance. *Adv. Funct. Mater.* **2012**, *22*, 4501−4510.
(23) Cai, J. G.; Lv, C.; Watanabe, A. Laser Direct Writing of High-Performance Flexible All-Solid-State Carbon Micro-Supercapacitors for An On-Chip Self-Powered Photodetection System. *Nano Energy* **2016**, *30*, 790−800.
(24) Wu, Z.-S.; Yang, S.; Zhang, L.; Wagner, J. B.; Feng, X.; Müllen, K. Binder-Free Activated Graphene Compact Films for All-Solid-State Micro-Supercapacitors with High Areal and Volumetric Capacitances. *Energy Storage Mater.* **2015**, *1*, 119−126.
(25) Lin, J.; Zhang, C.; Yan, Z.; Zhu, Y.; Peng, Z.; Hauge, R. H.; Natelson, D.; Tour, J. M. 3-Dimensional Graphene Carbon Nanotube Carpet-Based Microsupercapacitors with High Electrochemical Performance. *Nano Lett.* **2013**, *13*, 72−78.
(26) Dubal, D. P.; Kim, J. G.; Kim, Y.; Holze, R.; Lokhande, C. D.; Kim, W. B. Supercapacitors Based on Flexible Substrates: An Overview. *Energy Technol.* **2014**, *2*, 325−341.
(27) Qi, D.; Liu, Y.; Liu, Z.; Zhang, L.; Chen, X. Design of Architectures and Materials in In-Plane Micro-Supercapacitors: Current Status and Future Challenges. *Adv. Mater.* **2017**, *29*, 1602802.
(28) El-Kady, M. F.; Kaner, R. B. Scalable Fabrication of High-Power Graphene Micro-Supercapacitors for Flexible and On-Chip Energy Storage. *Nat. Commun.* **2013**, *4*, 1475−1483.
(29) Ji, J.; Li, Y.; Peng, W.; Zhang, G.; Zhang, F.; Fan, X. Advanced Graphene-Based Binder-Free Electrodes for High-Performance Energy Storage. *Adv. Mater.* **2015**, *27*, 5264−5279.
(30) Wu, Z. S.; Feng, X. L.; Cheng, H. M. Recent Advances in Graphene-Based Planar Micro-Supercapacitors for On-Chip Energy Storage. *Natl. Sci. Rev.* **2014**, *1*, 277−292.
(31) El-Kady, M. F.; Shao, Y.; Kaner, R. B. Graphene for Batteries, Supercapacitors and Beyond. *Nat. Rev. Mater.* **2016**, *1*, 16033−16046.
(32) Huang, P.; Lethien, C.; Pinaud, S.; Brousse, K.; Laloo, R.; Turq, V.; Respaud, M.; Demortiere, A.; Daffos, B.; Taberna, P. L.; Chaudret, B.; Gogotsi, Y.; Simon, P. On-Chip and Freestanding Elastic Carbon Films for Micro-Supercapacitors. *Science* **2016**, *351*, 691−695.
(33) Ling, Z.; Ren, C. E.; Zhao, M. Q.; Yang, J.; Giammarco, J. M.; Qiu, J.; Barsoum, M. W.; Gogotsi, Y. Flexible and Conductive Mxene Films and Nanocomposites with High Capacitance. *Proc. Natl. Acad. Sci. U. S. A.* **2014**, *111*, 16676−16681.
(34) Wu, Z. S.; Parvez, K.; Li, S.; Yang, S.; Liu, Z.; Liu, S.; Feng, X.; Müllen, K. Alternating Stacked Graphene-Conducting Polymer Compact Films with Ultrahigh Areal and Volumetric Capacitances for High-Energy Micro-Supercapacitors. *Adv. Mater.* **2015**, *27*, 4054−4061.
(35) Wu, Z. S.; Zheng, Y.; Zheng, S.; Wang, S.; Sun, C.; Parvez, K.; Ikeda, T.; Bao, X.; Müllen, K.; Feng, X. Stacked-Layer Heterostructure Films of 2D Thiophene Nanosheets and Graphene for High-Rate All-Solid-State Pseudocapacitors with Enhanced Volumetric Capacitance. *Adv. Mater.* **2017**, *29*, 1602960.
(36) Liu, Z.; Wu, Z. S.; Yang, S.; Dong, R.; Feng, X.; Müllen, K. Ultraflexible In-Plane Micro-Supercapacitors by Direct Printing of Solution-Processable Electrochemically Exfoliated Graphene. *Adv. Mater.* **2016**, *28*, 2217−2222.
(37) Ji, L. W.; Meduri, P.; Agubra, V.; Xiao, X. C.; Alcoutlabi, M. Graphene-Based Nanocomposites for Energy Storage. *Adv. Energy Mater.* **2016**, *6*, 1502159.
(38) Chen, L.; Zhou, G.; Liu, Z.; Ma, X.; Chen, J.; Zhang, Z.; Ma, X.; Li, F.; Cheng, H. M.; Ren, W. Scalable Clean Exfoliation of High-Quality Few-Layer Black Phosphorus for A Flexible Lithium Ion Battery. *Adv. Mater.* **2016**, *28*, 510−517.
(39) Kang, J.; Wells, S. A.; Wood, J. D.; Lee, J. H.; Liu, X.; Ryder, C. R.; Zhu, J.; Guest, J. R.; Husko, C. A.; Hersam, M. C. Stable Aqueous Dispersions of Optically and Electronically Active Phosphorene. *Proc. Natl. Acad. Sci. U. S. A.* **2016**, *113*, 11688−11693.
(40) Hanlon, D.; Backes, C.; Doherty, E.; Cucinotta, C. S.; Berner, N. C.; Boland, C.; Lee, K.; Harvey, A.; Lynch, P.; Gholamvand, Z.; Zhang, S.; Wang, K.; Moynihan, G.; Pokle, A.; Ramasse, Q. M.; Mcevoy, N.; Blau, W. J.; Wang, J.; Abellan, G.; Hauke, F.; et al. Liquid Exfoliation of Solvent-Stabilized Few-Layer Black Phosphorus for Applications Beyond Electronics. *Nat. Commun.* **2015**, *6*, 8563−8573.
(41) Park, C. M.; Sohn, H. J. Black Phosphorus and Its Composite for Lithium Rechargeable Batteries. *Adv. Mater.* **2007**, *19*, 2465−2468.
(42) Sun, J.; Lee, H. W.; Pasta, M.; Yuan, H.; Zheng, G.; Sun, Y.; Li, Y.; Cui, Y. A Phosphorene-Graphene Hybrid Material as A High-Capacity Anode for Sodium-Ion Batteries. *Nat. Nanotechnol.* **2015**, *10*, 980−985.
(43) Hao, C.; Yang, B.; Wen, F.; Xiang, J.; Li, L.; Wang, W.; Zeng, Z.; Xu, B.; Zhao, Z.; Liu, Z.; Tian, Y. Flexible All-Solid-State Supercapacitors Based on Liquid-Exfoliated Black-Phosphorus Nanoflakes. *Adv. Mater.* **2016**, *28*, 3194−3201.
(44) Zhong, Y. L.; Swager, T. M. Enhanced Electrochemical Expansion of Graphite for *in Situ* Electrochemical Functionalization. *J. Am. Chem. Soc.* **2012**, *134*, 17896−17899.
(45) Kang, J.; Wood, J. D.; Wells, S. A.; Lee, J. H.; Liu, X.; Chen, K. S.; Hersam, M. C. Solvent Exfoliation of Electronic-Grade, Two-Dimensional Black Phosphorus. *ACS Nano* **2015**, *9*, 3596−3604.
(46) Brent, J. R.; Savjani, N.; Lewis, E. A.; Haigh, S. J.; Lewis, D. J.; O'Brien, P. Production of Few-Layer Phosphorene by Liquid Exfoliation of Black Phosphorus. *Chem. Commun.* **2014**, *50*, 13338−13341.
(47) Voiry, D.; Yang, J.; Kupferberg, J.; Fullon, R.; Lee, C.; Jeong, H. Y.; Shin, H. S.; Chhowalla, M. High-Quality Graphene *via* Microwave Reduction of Solution-Exfoliated Graphene Oxide. *Science* **2016**, *353*, 1413−1416.
(48) Jover, J. F.; Lugo, R.; Toulhoat, H.; Simon, P.; De Bruin, T. Screening Methodology for The Efficient Pairing of Ionic Liquids and Carbonaceous Electrodes Applied to Electric Energy Storage. *J. Phys. Chem. C* **2014**, *118*, 864−872.
(49) Wang, Y. L.; Laaksonen, A.; Lu, Z. Y. Influence of Ionic Liquid Film Thickness on Ion Pair Distributions and Orientations at Graphene and Vacuum Interfaces. *Phys. Chem. Chem. Phys.* **2013**, *15*, 13559−13569.

DOI: 10.1021/acsnano.7b03288
ACS Nano 2017, 11, 7284−7292

(50) El-Kady, M. F.; Strong, V.; Dubin, S.; Kaner, R. B. Laser Scribing of High-Performance and Flexible Graphene-Based Electrochemical Capacitors. *Science* **2012**, *335*, 1326−1330.
(51) Wu, Z. S.; Parvez, K.; Feng, X.; Müllen, K. Graphene-Based In-Plane Micro-Supercapacitors with High Power and Energy Densities. *Nat. Commun.* **2013**, *4*, 2487−2494.
(52) Heon, M.; Lofland, S.; Applegate, J.; Nolte, R.; Cortes, E.; Hettinger, J. D.; Taberna, P. L.; Simon, P.; Huang, P. H.; Brunet, M.; Gogotsi, Y. Continuous Carbide-Derived Carbon Films with High Volumetric Capacitance. *Energy Environ. Sci.* **2011**, *4*, 135−138.
(53) Peng, Z. W.; Ye, R. Q.; Mann, J. A.; Zakhidov, D.; Li, Y. L.; Smalley, P. R.; Lin, J.; Tour, J. M. Flexible Boron-Doped Laser-Induced Graphene Microsupercapacitors. *ACS Nano* **2015**, *9*, 5868−5875.
(54) Gao, W.; Singh, N.; Song, L.; Liu, Z.; Reddy, A. L.; Ci, L.; Vajtai, R.; Zhang, Q.; Wei, B.; Ajayan, P. M. Direct Laser Writing of Micro-Supercapacitors on Hydrated Graphite Oxide Films. *Nat. Nanotechnol.* **2011**, *6*, 496−500.

DOI: 10.1021/acsnano.7b03288
ACS Nano 2017, 11, 7284−7292